SPONTANEOUS IGNITION OF HYDROCARBON–HYDROGEN–AIR MIXTURES

S. M. Frolov, S. N. Medvedev, V. Ya. Basevich, and F. S. Frolov

N. N. Semenov Institute of Chemical Physics
Russian Academy of Sciences
Moscow, Russia

Due to unique physical and chemical properties: low density (0.08 kg/m^3 at 300 K and 1 atm), wide flammability limits (from 4 to 75 %(vol.) in air), high laminar flame velocity (2.3 m/s at normal conditions), and very low ignition energy (0.02 mJ), hydrogen is considered as a candidate for partial or complete replacement of hydrocarbon fuels in power plants and transportation engines [1]. Despite spontaneous ignition and combustion characteristics of hydrogen and many individual hydrocarbons are fairly well studied, there is not much relevant data for hydrocarbon–hydrogen blends. As a matter of fact, only limited data are available on blended fuel combustion (e. g., methane–hydrogen [2], propane–hydrogen [3], kerosene–hydrogen [4, 5]) and spontaneous ignition (methane–hydrogen [6]). Surprisingly, the fact that hydrogen reactivity in air is not always higher than that of hydrocarbons, in particular, at low temperatures, is not discussed at all in the literature.

The objective of this paper is the theoretical study of the effect of hydrogen admixing on spontaneous ignition (self-ignition) of homogeneous and hybrid mixtures of heavy hydrocarbons (n-heptane and n-decane) in air based on the well-validated detailed reaction mechanism of n-hexadecane oxidation.

1 Chemical Reaction Mechanism

For modeling the effect of hydrogen additives to homogeneous and hybrid (with liquid droplets) mixtures of heavy hydrocarbons (n-heptane and n-decane) with air on self-ignition, a well-validated and relatively compact detailed reaction mechanism of n-hexadecane oxidation de-

veloped at N. N. Semenov Institute of Chemical Physics [7] has been used. This mechanism contains 2380 elementary processes that govern the reaction rate and the formation of basic intermediate and final products represented by 162 species. The mechanism has two essential features: (*i*) reactions of so-called double addition of oxygen (first, to the alkyl radical; then, to the isomerized form of the formed alkylperoxide radical) are lacking because the first addition is considered to be sufficient; and (*ii*) isomeric compounds and their derivative substances as intermediate species are not considered, because these means of oxidation are slower than through molecules and radicals of the normal structure. This mechanism was systematically validated for propane [8], *n*-butane [9], *n*-pentane [10], *n*-hexane [11], *n*-heptane [12], C_8–C_{10} alkanes [13], C_{11}–C_{16} alkanes [14], and hydrogen [15]. The major feature of this mechanism is the appearance of stages, viz., cool and blue flames during low-temperature self-ignition of alkane hydrocarbons and their blends.

Figures 1 and 2 show the performance of the mechanism on the example of homogeneous stoichiometric *n*-decane–air mixture. The calculations were made using the kinetic code KINET developed at N. N. Semenov Institute of Chemical Physics [16]. The code solves zero-dimensional time dependent equations of chemical kinetics coupled with the energy conservation equation for isobaric conditions.

Figure 1 presents typical calculated time dependences of temperature during spontaneous ignition of alkane hydrocarbons, which are characteristic for low and high initial temperatures. The first stepped increase for the relatively low initial temperature $T_0 = 588$ K at $t \sim 1.27$ s is related to the appearance of the cool flame. The blue flame then appears after a lapse of about 0.28 s; the hot flame then appears at approximately 1.57 s and the temperature increases to 2500 K and higher. The stages of spontaneous ignition, i. e., stepwise appearance of cool, blue, and hot flames, occur as follows. The acceleration of the reaction in the cool flame is the consequence of branching during decomposition of alkyl hydroperoxide (here, alkyl hydroperoxide $C_{10}H_{21}O_2H$) with the formation of hydroxyl and oxyradical. The appearance of the blue flame is the consequence of branching because of the decomposition of hydrogen peroxide H_2O_2. These stages result in the phenomenon of the negative temperature coefficient (NTC) of the reaction rate; the overall self-ignition delays at a higher initial temperature appear to be

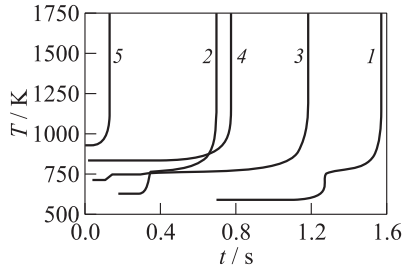

Figure 1 Spontaneous ignition of stoichiometric n-decane–air mixture: predicted time histories of temperature at $T_0 = 588$ (*1*), 625 (*2*), 714 (*3*), 833 (*4*), and 930 K (*5*), at initial pressure $P_0 = 1$ atm

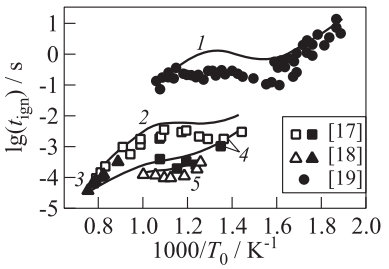

Figure 2 Spontaneous ignition of stoichiometric n-decane–air mixture: comparison of measured (points [17–19]) and calculated (curves) self-ignition delays at different temperatures and pressures: *1* — $P = 1$ atm; *2* — 12; *3* — 13; *4* — 50; and *5* — $P = 80$ atm

greater than at a low temperature. This effect is clearly seen in Fig. 1. Note that in the calculations, the overall self-ignition delay time $t_{\rm ign}$ was determined as the time taken for the temperature growth rate to attain the value of 10^7 K/s. Other possible definitions (10^6 K/s and $\max(dT/dt)$) were proved to give very similar results for $t_{\rm ign}$. Figure 2 compares calculated (curves) and measured (points) overall self-ignition delays $t_{\rm ign}$ of n-decane–air mixture for various initial temperatures and pressures. The points on the graph correspond to the experimental data of [17] for pressures of 12 and 50 atm, [18] for pressures of 13 and 80 atm, and [19] for a pressure of 1 atm. It follows from Fig. 2 that the detailed reaction mechanism of n-decane oxidation provides satisfactory agreement with available experimental data on overall self-ignition delays in wide ranges of initial temperature and pressure.

2 Model of Droplet Self-Ignition and Combustion

The liquid droplet (index d) is assumed to be a sphere of diameter $d = 2r_s$ and occupy the region $0 < r < r_s$ at time t (index s relates to drop surface). The droplet size is allowed to vary in time due to

thermal expansion and liquid vaporization processes. Therefore, r_s is treated as the moving boundary.

The gas phase (index g) is assumed to occupy region $r_s < r < R$ where R is the effective half-distance between droplets in gas–droplet suspension. This parameter can be found based on the simple formula [20]:

$$R = r_{s0}\left(\frac{\rho_d}{\eta}\right)^{1/3} = r_{s0}\left(\frac{\rho_d}{\rho_g \Phi \phi_{\rm st}}\right)^{1/3} \tag{1}$$

where index 0 denotes the initial value; η is the mass content of liquid in the unit volume of droplet suspension; ρ is the density; Φ is the fuel–air ratio; and $\phi_{\rm st}$ is the stoichiometric fuel–air ratio ($\phi_{st} \approx 0.06$ for heavy hydrocarbon fuels).

The set of governing equations includes [20] the continuity and energy equations for liquid, and continuity, species continuity, and energy equations for gas, supplemented with the equation of state, initial and boundary conditions, and the internal boundary conditions at $r = r_s$ for tailoring the temperature fields in liquid and gas. Molecular transport processes in liquid and gas as well as the corresponding specific heats were taken from [21].

The set of equations was integrated numerically using DROP code developed at N. N. Semenov Institute of Chemical Physics. Applied in the code is a nonconservative finite-difference scheme and adaptive moving grid. The computational error was continuously monitored by checking balances of C and H atoms as well as energy balance at each time step.

The model described above was thoroughly validated against experimental data on droplet self-ignition and combustion for various liquid hydrocarbons using the detailed reaction mechanism of n-hexadecane oxidation [7]. As an example, Fig. 3 compares the calculated (curve) and measured (points [22, 23]) dependences of the overall ignition delay time $t_{\rm ign}$ for n-heptane droplets. The definition of $t_{\rm ign}$ was the same as for the homogeneous mixtures but the criterion 10^7 K/s for the temperature growth rate was applied to the maximum gas temperature $T_{g,\max}(t)$. As can be seen, the overall self-ignition delay time increases sharply at low pressures. Furthermore, Fig. 4 compares the calculated (curves) and measured (points from [24]) ignition delay times of cool flame appearance ($t_{\rm cf}$) and overall self-ignition delay time ($t_{\rm ign}$) for n-decane

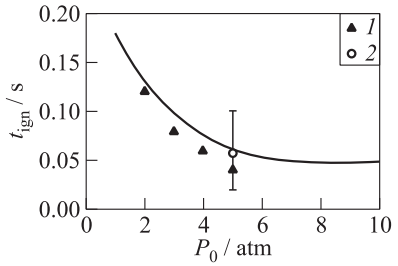

Figure 3 Predicted (curve) and measured (points) self-ignition delay time $t_{\rm ign}$ vs. pressure for n-heptane droplets with $d_0 = 700$ μm at $T_0 = 1000$ K: *1* — $d_0 = 700$–750 μm and $T_0 = 1000$ K [22]; and *2* — $d_0 = 700$ μm and $T_0 = 940$ K [23] (the vertical bar indicates the scatter in experimental data [2])

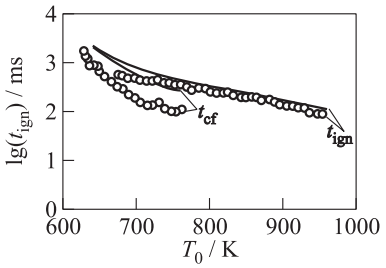

Figure 4 Predicted (curves) and measured (points [24]) delay times of cool flame ($t_{\rm cf}$) and hot flame ($t_{\rm ign}$) appearance vs. initial temperature for a single n-decane drop in air: $d_0 = 700$ μm and $P_0 = 1$ atm

droplets of initial diameter 700 μm at different initial temperatures and pressure $P_0 = 1$ atm. The delay time of cool flame appearance ($t_{\rm cf}$) was defined as the time taken for the maximum gas temperature $T_{g,\max}$ to attain the inflection point at the first stepwise temperature variation in the $T_{g,\max}$–t plane. Clearly, the model predicts correctly not only qualitative features of droplet self-ignition phenomenon but also provides satisfactory quantitative information. Note that cool flames during self-ignition of liquid sprays were first observed experimentally long ago [25].

3 Spontaneous Ignition of Homogeneous Hydrocarbon–Hydrogen–Air Blends

The reaction mechanism [7] was first used to study the effect of hydrogen addition on the self-ignition delay time of homogeneous hydrocarbon–air mixtures. The calculations of mixture self-ignition and volumetric combustion were performed using KINET code.

Figure 5 shows the predicted dependences of overall self-ignition delays on temperature for homogeneous stoichiometric n-heptane–air

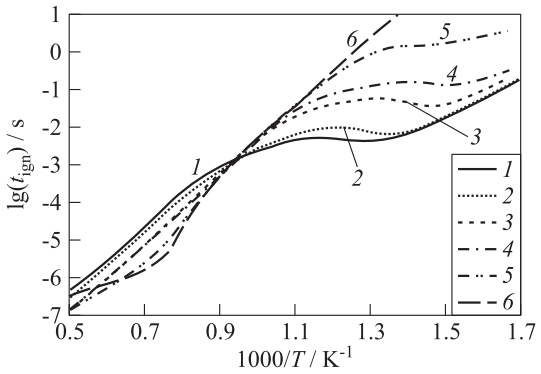

Figure 5 Predicted dependences of self-ignition delays on temperature for stoichiometric homogeneous C_7H_{16}–H_2–air mixtures with different hydrogen content: *1* — 0 %(vol.), *2* — 50, *3* — 90, *4* — 95, *5* — 99, and *6* — 100 %(vol.); pressure $P_0 = 15$ atm

mixtures with different content of hydrogen (from 0 to 100 %(vol.) at pressure $P_0 = 15$ atm. At $T_0 \approx 1050$ K, the self-ignition delays of n-heptane–air and hydrogen–air mixtures are seen to be the same. At $T_0 < 1050$ K, addition of hydrogen to n-heptane–air mixture increases the self-ignition delay, whereas at $T_0 > 1050$ K, decreases it. Note that even in the mixtures with high amount of hydrogen (e. g., 99 %(vol.)), the effect of NTC of reaction rate is clearly seen in Fig. 5.

4 Spontaneous Ignition of Hybrid Hydrocarbon (Droplets) – Hydrogen–Air Mixtures

The reaction mechanism [7] was then used to study the effect of hydrogen addition on the self-ignition delay time of hybrid hydrocarbon (droplets) – hydrogen–air mixtures. The calculations of ignition and combustion of such mixtures were performed using DROP code.

Shown in Fig. 6 are the predicted time histories of the maximum gas temperature at self-ignition of n-heptane (Fig. 6*a*) and n-decane (Fig. 6*b*) droplet suspensions in air mixed with 7.5 %(vol.) hydrogen (solid curves) and in pure air (dashed curves) at $P_0 = 20$ atm and different initial temperatures. It is clearly seen that hydrogen addition

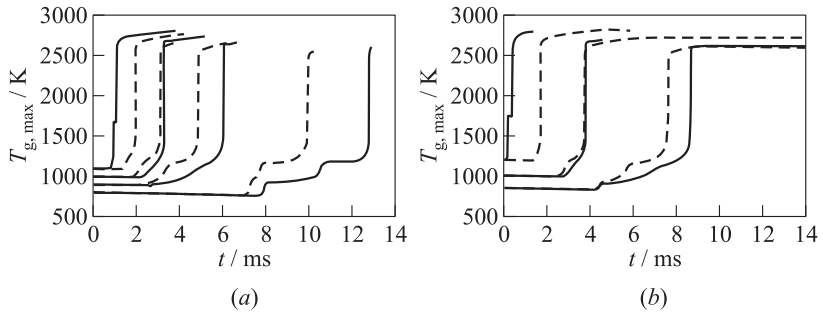

Figure 6 Predicted time histories of the maximum gas temperature $T_{g,\max}$ in the stoichiometric mixtures n-heptane (droplets) – hydrogen–air (a) and n-decane (droplets) – hydrogen–air (b) at different initial temperatures and different initial hydrogen content: 7.5 %(vol.) H_2 (solid curves) and 0 %(vol.) H_2 (dashed curves); drop diameter $d_0 = 60$ μm and $P_0 = 20$ atm

affects not only the overall self-ignition delay time $t_{\rm ign}$ but also the duration of intermediate stages of multistage self-ignition (cool and blue flames).

At a relatively low temperature (e. g., at $T_0 = 800$ K), the duration of cool and blue flame stages changes considerably. This indicates that molecular hydrogen deactivates active intermediate radicals participating in the channels of chain origination, propagation, and branching. Nevertheless, similar to homogeneous mixtures, at $T_0 < 1050$ K, the self-ignition delay time in the hydrogen-containing hybrid mixtures increases as compared to the mixtures without hydrogen, whereas at $T_0 > 1050$ K, it decreases. One has to keep in mind that Fig. 6 relates to the self-ignition of hybrid rather than homogeneous mixture. At self-ignition of liquid droplets, the temperature and fuel vapor concentration in the vicinity of the droplet surface are highly nonuniform. Moreover, self-ignition of fuel vapor occurs in the region where the gas temperature is lower than its value at a large distance from the droplet surface and the fuel vapor – air mixture is essentially fuel lean [20].

The detailed analysis of various physical and chemical processes in the vicinity to the droplet surface reveals several interesting features of hybrid mixture self-ignition. For example, Fig. 7 shows the time

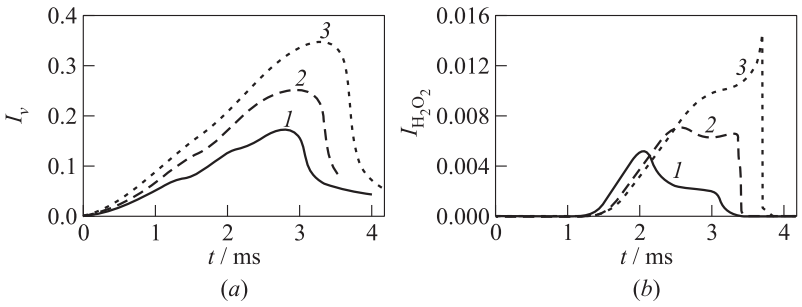

Figure 7 Predicted time histories of the normalized mass contents of fuel vapor (a) and hydrogen peroxide (b) around a droplet in uniform stoichiometric n-heptane droplet suspension at different initial volumetric H_2 content: *1* — 0%, *2* — 7.5%, and *3* — 14.5%; $d_0 = 60$ μm and $P_0 = 20$ atm

histories of the normalized mass content of fuel vapor I_v (Fig. 7a) and hydrogen peroxide $I_{H_2O_2}$ (Fig. 7b) in the sphere of radius R around the fuel droplet in uniform stoichiometric n-heptane droplet suspension (R is the effective half-distance between droplets in gas–drop suspension, see above). The normalized mass content of the ith species in the gas phase is defined as

$$I_i(t) = m_0^{-1} \int\limits_{r_s(t)}^{R} 4\pi\xi^2 \rho_i(\xi, t)\, d\xi \tag{2}$$

where m_0 is the initial mass of the fuel droplet and ρ_i is the partial density of the ith species.

The overall self-ignition delay time in Fig. 7 associated with a sharp depletion of fuel vapor and hydrogen peroxide is seen to increase with hydrogen content. Also, addition of increasing amounts of hydrogen to the gas–droplet suspension results in faster droplet vaporization (caused by high hydrogen specific heat and diffusivity) and larger amounts of fuel vapor and hydrogen peroxide accumulated near the droplet before self-ignition occurs. Such a behavior of the overall self-ignition delay time is caused by reactions of molecular hydrogen with the intermediate products of n-heptane oxidation leading to the formation of less active radicals like HO_2.

5 Concluding Remarks

The detailed reaction mechanism of n-hexadecane oxidation in air was used to simulate self-ignition of stoichiometric homogeneous hydrocarbon–hydrogen–air mixtures and hybrid mixtures of hydrocarbon droplets with hydrogen and air at different initial temperature, pressure and volumetric hydrogen content. Two hydrocarbons were investigated: n-heptane and n-decane.

It has been shown that the reactivity of hydrogen-containing mixtures is not always higher than that of the pure hydrocarbon–air mixture. At approximately $T_0 < 1050$ K, addition of hydrogen to hydrocarbon–air mixture was shown to increase the overall self-ignition delay time, i. e., hydrogen plays the role of self-ignition inhibitor. In these conditions, with the increase of hydrogen content in homogeneous and hybrid mixtures, the duration of the cool-flame and blue-flame reaction stages was shown to change drastically and even to degenerate. This phenomenon is caused by reactions of molecular hydrogen with the intermediate products of hydrocarbon oxidation leading to the formation of less active species like HO_2 radical hindering chain-branching processes. Nevertheless, at approximately $T_0 > 1050$ K, hydrogen addition was shown to decrease the overall self-ignition delay time thus indicating that hydrogen serves as self-ignition promoter. These findings have to be taken into account when discussing the perspectives of practical applications of fuels blended with hydrogen.

Acknowledgments

This work was supported by the Program No. 26 “Combustion and Explosion” of the Presidium of the Russian Academy of Sciences.

References

1. Verhelst, S., and T. Wallner. 2009. Hydrogen-fueled internal combustion engines. *Prog. Energy Combust. Sci.* 35:490–527.
2. Zhanga, Y., J. Wu, and S. Ishizuka. 2009. Hydrogen addition effect on laminar burning velocity, flame temperature and flame stability of a planar and a curved CH_4–H_2–air premixed flame. *Int. J. Hydrogen Energy* 34:519–527.

3. Cheng, R. K., D. Littlejohn, P. A. Strakey, and T. Sidwell. 2009. Laboratory investigations of a low-swirl injector with H_2 and CH_4 at gas turbine conditions. *Proc. Combust. Inst.* 32(II):3001–3009.

4. Frenillota, J. P., G. Cabota, M. Cazalens, B. Renoua, and M. A. Boukhalfa. 2009. Impact of H_2 addition on flame stability and pollutant emissions for an atmospheric kerosene/air swirled flame of laboratory scaled gas turbine. *Int. J. Hydrogen Energy* 34:3930–3944.

5. Burguburu, J., G. Cabot, B. Renou, A. M. Boukhalfa, and M. Cazalens. 2011. Effects of H_2 enrichment on flame stability and pollutant emissions for a kerosene/air swirled flame with an aeronautical fuel injector. *Proc. Combust. Inst.* 33:2927–2935.

6. Cheng, R. K., and A. K. Oppenheim. 1984. Autoignition in methane–hydrogen mixtures. *Combust. Flame* 58:125–139.

7. http://ru.combex.org/news-archive.htm (accessed June 15, 2014).

8. Basevich, V. Y., A. A. Belyaev, and S. M. Frolov. 2007. The mechanisms of oxidation and combustion of normal alkane hydrocarbons: The transition from C_1–C_3 to C_4H_{10}. *Rus. J. Phys. Chem. B* 2(5):477–484.

9. Basevich, V. Y., V. I. Vedeneev, S. M. Frolov, and L. B. Romanovich. 2006. Nonextensive principle to construct oxidation and combustion mechanisms of normal alkane hydrocarbons: The transition from C_1–C_2 to C_3H_8. *Rus. J. Chem. Phys.* 25(11):87.

10. Basevich, V. Y., A. A. Belyaev, and S. M. Frolov. 2009. Mechanisms of the oxidation and combustion of normal alkanes: The transition from C_1–C_4 to C_5H_{12}. *Rus. J. Phys. Chem. B* 3:629.

11. Basevich, V. Y., A. A. Belyaev, and S. M. Frolov. 2010. Mechanisms of the oxidation and combustion of normal alkanes: Transition from C_1–C_5 to C_6H_{14}. *Rus. J. Phys. Chem. B* 4:634.

12. Basevich, V. Y., A. A. Belyaev, V. S. Posvyanskii, and S. M. Frolov. 2010. Mechanism of the oxidation and combustion of normal paraffin hydrocarbons: Transition from C_1–C_6 to C_7H_{16}. *Rus. J. Phys. Chem. B* 4:985.

13. Basevich, V. Y., A. A. Belyaev, S. N. Medvedev, V. S. Posvyanskii, and S. M. Frolov. 2011. Oxidation and combustion mechanisms of paraffin hydrocarbons: Transfer from C_1–C_7 to C_8H_{18}, C_9H_{20}, and $C_{10}H_{22}$. *Rus. J. Phys. Chem. B* 5(6):974–990.

14. Basevich, V. Ya., A. A. Belyaev, V. S. Posvyanskii, and S. M. Frolov. 2013. Mechanisms of the oxidation and combustion of normal paraffin hydrocarbons: Transition from C_1–C_{10} to C_{11}–C_{16}. *Rus. J. Phys. Chem. B* 7(2):161–169.

15. Frolov, S. M., S. N. Medvedev, V. Ya. Basevich, and F. S. Frolov. 2013. Self-ignition of hydrocarbon–hydrogen–air mixtures. *Int. J. Hydrogen Energy* 38:4177–4184.
16. Lidskii, B. V., M. G. Neuhaus, V. Y. Basevich, and S. M. Frolov. 2003. On calculation of laminar flame propagation with regard for multicomponent diffusion. *Rus. J. Chem. Phys.* 22(3):51.
17. Pfahl, U., K. Fieweger, and G. Adomeit. 1996. Self-ignition of diesel-relevant hydrocarbon–air mixtures under engine conditions. *26th Symposium (International) on Combustion Proceedings*. Pittsburgh: Combustion Institute. 781.
18. Zhukov, V. P., V. A. Sechenov, and A. Y. Starikovskii. 2008. Autoignition of n-decane at high pressure. *Combust. Flame* 153:130.
19. Troshin, K. Y. 2008. Experimental study of the ignition of n-hexane- and n-decane-based surrogate fuels. *Rus. J. Chem. Phys.* 2(3):419–425.
20. Frolov, S. M., V. Y. Basevich, F. S. Frolov, A. A. Borisov, V. A. Smetanyuk, K. A. Avdeev, and A. N. Gotz. 2009. Correlation between drop vaporization and self-ignition. *Rus. J. Chem. Phys.* 28(5):3–18.
21. Reid, R. C., J. M. Prausnitz, and T. K. Sherwood. 1977. *The properties of gases and liquids*. New York, N.Y., USA: McGrow-Hill. 741 p.
22. Tanabe, M., T. Bolik, C. Eigenbrod, and H. J. Rath. 1996. Spontaneous ignition of liquid droplets from a view of non-homogeneous mixture formation and transient chemical reactions. *Proc. Combust. Inst.* 26:1637–1643.
23. Schnaubelt, S, O. Moriue, T. Coordes, C. Eigenbrod, and H. J. Rath. 2000. Detailed numerical simulations of the multistage self-ignition process of n-heptane, isolated droplets and their verification by comparison with microgravity experiments. *Proc. Combust. Inst.* 28:953.
24. Moriue, O, C. Eigenbrod, H. J. Rath, J. Sato, K. Okai, M. Tsue, and M. Kono. 2000. Effects of dilution by aromatic hydrocarbons on staged ignition behavior of n-decane droplets. *Proc. Combust. Inst.* 28(1):969–975.
25. Sokolik, A. S., and V. Y. Basevich. 1954. On the kinetic nature of self-ignition in diesel engine conditions. *Sov. J. Phys. Chem.* 28:1935.